

Frequency behavior of Raman coupling coefficient in glasses

N.V. Surovtsev¹, A.P. Sokolov²

¹ *Institute of Automation and Electrometry, Russian Academy of Sciences,
pr.Ak.Koptyuga 1, Novosibirsk, 630090, Russia*

² *Department of Polymer Science, University of Akron, Akron, OH 44325 -
3909*

(October 25, 2018)

Low-frequency Raman coupling coefficient $C(\nu)$ of 11 different glasses is evaluated. It is shown that the coupling coefficient demonstrates a universal linear frequency behavior $C(\nu) \propto (\nu/\nu_{BP} + B)$ near the boson peak maximum, ν_{BP} . Frequency dependence of $C(\nu)$ allows to separate the glasses studied into two groups: the first group has a frequency independent contribution $B \sim 0.5$, while the second one has $B \sim 0$. It was found that $C(\nu)$ demonstrates a superlinear behavior at very low frequencies. This observation suggests vanishing of the coupling coefficient when frequency tends to zero. The results are discussed in terms of the vibration wavefunction that combines features of localized and extended modes.

I. INTRODUCTION

One of the most interesting topics in solid state physics is the nature of the low-frequency (0.1-3 THz) collective vibrations in glasses. While these frequencies are in the range of acoustic excitations, there are experimental evidences that the vibrations are not pure acoustic plane waves and their density of vibrational states $g(\nu)$ does not follow the Debye behavior ($\propto \nu^2$, where ν is a frequency). A maximum in $g(\nu)/\nu^2$ that appears at some frequency ν_{BP} is usually called the boson peak. Vibrations around the boson peak can be studied by several experimental techniques: low-temperature specific heat and thermal conductivity¹, inelastic neutron² and X-ray^{3,4} scattering, infrared absorption⁵ and Raman scattering⁶. In the case of the low-frequency Raman spectroscopy, the density of vibrational states appears in the light scattering spectrum via the so-called light-vibration coupling coefficient, $C(\nu)$,⁷

$$I(\nu) = C(\nu) g(\nu) \frac{n+1}{\nu} \quad (1)$$

where $I(\nu)$ is the Raman intensity for the Stokes side of the spectrum, and n is the Bose factor.

A knowledge of $C(\nu)$ and an understanding of its frequency dependence have significant importance for the topic of the low-frequency vibrations. First of all, a knowledge of $C(\nu)$ provides a relatively simple method to extract the vibrational density of states from a Raman experiment. Secondly, the light-vibration coupling coefficient contains information on the vibrational

wavefunction⁷ and, therefore, can be used as a test of different models.

Two classical models suggested for the description of $C(\nu)$ lead to different predictions: (i) Shuker and Gammon⁷ assumed that vibrations are localized on a distance much shorter than the light wavelength and predicted $C(\nu) = const$, while (ii) Martin and Brenig⁸ have demonstrated that a polarizability disorder mechanism applied to slightly damped acoustic waves leads to $C(\nu) \sim \nu^2$ behavior at low frequencies and a peak at higher frequencies, related to a correlation length of the polarizability fluctuations. It was shown that quasi-plane acoustic waves with finite mean free path, ℓ , will also contribute to the low-frequency Raman spectrum with $C(\nu) \sim \nu^2$, when $\ell^{-1} \propto \nu^4$, Ref.^{6,9}, or with $C(\nu) = const$, when $\ell^{-1} \propto \nu^2$, Ref.^{9,10}.

There are a few challenges for experimental evaluation of the true vibration coupling coefficient: Very low temperature data for both - Raman spectra and $g(\nu)$ - should be used in order to avoid a quasielastic contribution (fast relaxation)^{6,11}; it is not obvious whether all vibrations at one frequency contribute to the Raman spectra with the same $C(\nu)$, or there are different kinds of vibrations and each contributes with its own $C(\nu)$. A comparison of the low-temperature low-frequency Raman spectra of glasses with the total $g(\nu)$ obtained from low-temperature specific heat or inelastic neutron data has demonstrated that the coupling coefficient appears to vary nearly linearly with frequency¹²⁻¹⁶.

However, this comparison did not consider the possibility that two different kinds of vibrational excitations could co-exist around the boson peak. Although most of the authors at present accept the idea that the vibrations around the boson peak are strongly hybridized and can not be easily separated, the question is not yet completely settled. This question became especially important in the light of the results of Hyper-Raman scattering experiments¹⁷. The existence of differences in the behavior of THz spectra in Raman and Hyper-Raman scattering experiments was interpreted as evidence of the co-existence of two types of vibrational excitations. Also, there are theoretical approaches describing the THz dynamics of glasses as a co-existence of two different types of vibrations in this spectral range (for example,^{18,19}). In this case, the Raman coupling coefficient can lose its good physical meaning²⁰. One of the strong arguments in favor of the existence of a single type of vibrational exci-

tation could be the universal behavior of $C(\nu)$ for glasses with various structures. This universality suggests that the two hypothetical types of vibrations are interrelated.

A detailed analysis performed for silica glass has shown that $C(\nu)$ varies linearly with frequency,

$$C(\nu) = A(\nu/\nu_{BP} + B) \quad (2)$$

in the range 10-50 cm^{-1} .²¹ This result was interpreted in²¹ as an evidence that the coupling coefficient extrapolates to a nonvanishing value in the limit $\nu \rightarrow 0$. However, it was shown in²² that the coupling coefficient demonstrates a superlinear behavior just below 10 cm^{-1} , i.e. the observed linear behavior can not be extrapolated to zero frequency. It would be very important to know whether this behavior is general also for other glasses.

The present contribution analyzes the frequency behavior of the coupling coefficient in a broad set of different glasses, strong and fragile, covalently and ionically bonded, low molecular weight and polymeric. It is shown that all glasses demonstrate the linear behavior of $C(\nu)$ (eq.(2)) around the boson peak frequency. One of the most striking results is that there are two groups of glasses. One has a frequency independent contribution B with a universal value ~ 0.5 , while the second group of glasses has $B \approx 0$. An interpretation of the results is proposed and a correlation with low-temperature thermal conductivity is found.

II. RESULTS

The density of vibrational states must be known in order to extract the Raman coupling coefficient (see, eq.(1)). It has been shown^{6,11,23} that relaxation-like processes give significant contribution to the Raman spectra and $g(\nu)$ at frequencies below the boson peak even at temperatures as low as 50 K. Thus, experimental data obtained at T below 50 K should be used for extracting vibrational $g(\nu)$. Two experimental techniques provide information on $g(\nu)$: inelastic neutron scattering² and measurements of low-temperature specific heat¹. The latter has a few advantages: (i) the number of glasses for which specific heat data are available is much larger than the number of glasses for which inelastic neutron scattering data are available; (ii) the density of states calculated from low-temperature specific heat data corresponds to a very low temperature, where usually no neutron data are available. While in the past only a phenomenological analysis was available for extraction of the coupling coefficient from the comparison of the specific heat and Raman data (for example,^{13,24}), recently it was shown that the integral equation for specific heat temperature dependence can be solved numerically and therefore the density of vibrational states may now be obtained from heat capacity measurements²².

SiO₂. The low-temperature density of states of Heralux silica glass was calculated from the specific heat

data published in²⁵ using the procedure described in details in²². It was shown in this work that the density of states obtained from the specific heat data is in excellent agreement with the one measured by inelastic neutron scattering^{21,26}. Low-temperature polarized Raman data from Heralux glass were taken from²⁷ ($T=7$ K) and depolarized data taken from²⁸ ($T=10$ K). The Raman coupling coefficient for the density of states evaluated from the specific heat data is in good agreement with that calculated from comparison of the Raman and neutron data^{12,21} (Fig.1). Note that the deviation of $C(\nu)$ of Ref.²¹ in the high-frequency part is related to different kinds of silica glasses used for light and neutron scattering. The difference between the results reported in¹² and those reported in²² at very low-frequencies is related to the presence of a quasielastic contribution at $T=50$ K (lowest temperature used in Ref.¹²) in the range $\nu < 10$ cm^{-1} . This difference stresses the importance of using very low temperature data for estimates of the vibrational $C(\nu)$.

Fig.1 demonstrates (see also the inset) that in the frequency range 10-40 cm^{-1} the coupling coefficient varies linearly with frequency, $C(\nu) \propto (\nu/\nu_{BP} + B)$. The coupling coefficient is proportional to frequency in the range from ~ 40 cm^{-1} up to ~ 120 cm^{-1} . A superlinear behavior is observed below 10 cm^{-1} . In the Raman experiment of Ref.²⁷, the signal in the range 7-8 cm^{-1} was so weak that it was not possible to detect it. In this case only an estimate of the upper limit of the signal is available. This estimate was used for the calculation of the upper limit for $C(\nu)$ at frequencies 7-8 cm^{-1} . The open circles in Fig. 1 show the upper limit of the coupling coefficient (for the polarized spectrum). Thus, it is very likely, that the linear behavior of $C(\nu)$ observed in²¹ is restricted to frequencies above 10 cm^{-1} , but the coupling coefficient has another frequency dependence for $\nu < 10$ cm^{-1} . Also it follows from the data of¹² that $C(\nu)$ increases faster than linear at $\nu < 10$ cm^{-1} . Further measurements of Raman scattering in silica glass at low frequencies and low temperatures (< 10 K) are needed in order to clarify the frequency behavior of the coupling coefficient at $\nu < 10$ cm^{-1} .

B₂O₃. The density of states was calculated from the specific heat data of the D5 sample published in²⁹. The specific heat data of²⁹ were extended above $T=20$ K by the results published in³⁰ (the results of²⁹ show that the specific heat data of different boron oxide glasses collapse to a single curve above ~ 15 K). Raman data measured at $T=15$ K were taken from³¹ (the sample used in³¹ is identical to D5 from²⁹ as it follows from Ref.³²). The calculated coupling coefficient (Fig.2) is in good agreement with the one published in¹⁸. Fig2. shows that the frequency behavior of the coupling coefficient in B₂O₃ glass is linear below 30 cm^{-1} and is proportional to $\nu^{0.5}$ above 30 cm^{-1} .

Se. The density of vibrational states of Se glass was calculated from specific heat data published in^{33,34}. In the range 10-60 cm^{-1} , this calculation is in fair agree-

ment with the results of neutron scattering at $T=100$ K published in³⁵. The depolarized Raman spectrum of Se glass at $T=6$ K was taken from¹³. The coupling coefficient (Figure 3) was calculated using density of states evaluated from both, specific heat and neutron scattering data. It is linear in the range $5-20$ cm^{-1} and varies more strongly than linearly above this range. The superlinear behavior of $C(\nu)$ also appears below 5 cm^{-1} .

CKN. The vibrational density of states was calculated from the specific heat data published in³⁶. The specific heat in this work was measured up to 8.5 K. It is expected that the vibrational density of states found will be valid in a frequency range up to about 20 cm^{-1} (see²²). The low-frequency Raman spectrum at $T=6$ K was taken from³⁷. The density of states at $T=252$ K of CKN glass was measured in³⁸. Since the density of states does not demonstrate significant temperature variations for $\nu > 10$ cm^{-1} Ref.³⁸, the coupling coefficient at $T=200$ K was calculated using the Raman data at $T=200$ K (data from³⁷) and neutron scattering data of³⁸ (no correction for the Debye-Waller factor was done for $S(Q, \nu)$). The two estimates of the coupling coefficient (from neutron and specific heat experiments, Fig.3) show good agreement in the range $10-30$ cm^{-1} , while the presence of the fast relaxation below 10 cm^{-1} is clear at $T=200$ K. The coupling coefficient reveals a linear frequency behavior in the range $10-22$ cm^{-1} and the stronger dependencies below 10 cm^{-1} and above 35 cm^{-1} .

As₂S₃. The density of states was calculated from the specific heat data published in¹⁴ (data for the annealed sample). The evaluated density of states in the range $10-60$ cm^{-1} is in fair agreement with $g(\nu)$ obtained from inelastic neutron scattering measurements³⁹ at room temperature. A low-temperature depolarized Raman spectrum of the As₂S₃ glass was measured in¹³. The values of $C(\nu)$ from that work (Fig.4) show that the coupling coefficient is proportional to ν in the range $5-60$ cm^{-1} .

GeO₂. Low-temperature low-frequency Raman data and specific heat data for GeO₂ glass were taken from⁴⁰. The density of states was calculated from the specific heat. The values of $C(\nu)$ (Fig.4) derived from that data show that $C(\nu)$ is nearly proportional to ν for the whole frequency range $10-50$ cm^{-1} .

GeSe₂. Inelastic neutron scattering data and low-temperature specific heat data for GeSe₂ glass are presented in⁴¹. Our evaluation of the vibrational density of states from the low-temperature specific heat (measured up to 18 K) is in good agreement with room temperature neutron data in the range $10-50$ cm^{-1} . This agreement suggests that a contribution of the fast relaxation in this frequency range is negligible already at ambient conditions. A room temperature Raman spectrum of GeSe₂ glass was taken from⁴². The spectrum measured in this work shows a well defined peak already at room temperature, supporting the contention that the quasielastic contribution is well suppressed at frequencies corresponding to the boson peak maximum. The coupling coefficient was calculated from a comparison of Raman and neutron

scattering data at room temperature (Fig.4). This calculation demonstrates nearly linear frequency behavior of $C(\nu)$ in the whole frequency range $8-90$ cm^{-1} .

(Ag₂O)_{0.14}(B₂O₃)_{0.86}. Vibrational density of states of a (Ag₂O)_{0.14}(B₂O₃)_{0.86} glass was calculated from the specific heat data of⁴³. Specific heat data were measured up to 18 K in this work. Since the low-temperature specific heat coincides with that of B₂O₃ glass for $T > 10$ K⁴³, we extended the data of the (Ag₂O)_{0.14}(B₂O₃)_{0.86} glass to higher temperature using the data from the B₂O₃ glass. The extended data allowed us to calculate the density of states for higher frequency. A low-temperature depolarized Raman spectrum recorded at $T=20$ K was taken from⁴³. The derived coupling coefficient of (Ag₂O)_{0.14}(B₂O₃)_{0.86} glass (Fig.4) is linear in the range $10-60$ cm^{-1} and slightly superlinear above this range.

Polystyrene (PS). The density of vibrational states of PS glass was calculated from the specific heat data published in^{30,44}. A low-temperature depolarized Raman spectrum (at $T=6$ K) was taken from⁴⁵. In the frequency range $8-90$ cm^{-1} , $C(\nu)$ calculated from these data (Fig.5) agrees well with the coupling coefficient obtained earlier by direct comparison of neutron and Raman scattering data at $T=35$ K (from¹²). The contribution of the fast relaxation⁴⁵ at $T=35$ K is responsible for the difference between the two estimates of coupling coefficient at frequencies below 8 cm^{-1} . The coupling coefficient in PS glass (Fig.5) varies linearly with ν in the range $5-40$ cm^{-1} and superlinear above and below this range.

Polycarbonate (PC). The coupling coefficient at $T=15$ K for PC glass was found in¹⁰ by direct comparison of neutron and Raman scattering spectra. It is linear in the range $5-50$ cm^{-1} and superlinear above this range (Fig.5).

Polymethylmethacrylate (PMMA). Calculation of vibrational density of states of PMMA glass was done from the specific heat data published in³⁰. A low-temperature Raman spectrum was measured in⁴⁶. $C(\nu)$ obtained from that data (Fig.5) agrees well with the coupling coefficient found in⁴⁷ from comparison of neutron and Raman scattering spectra at $T=30$ K. $C(\nu)$ varies linearly with ν in the range $7-30$ cm^{-1} and has a stronger frequency dependence above this range.

III. GENERAL FEATURES OF $C(\nu)$

In this section some general properties of the Raman coupling coefficient will be discussed. The goal is to reveal features that are universal or different for the glasses analyzed.

The results presented in the previous section indicate that the frequency behavior of coupling coefficient can be considered in three frequency ranges: significantly below the frequency of the boson peak maximum, ν_{BP} ; around ν_{BP} and significantly above ν_{BP} . The comparison will

be done with the frequency axis scaled to ν_{BP} . The frequency ν_{BP} was defined as the position of the maximum in the curve $g(\nu)/\nu^2$. Table 1 presents for the glasses under discussion the values of ν_{BP} defined in this way.

Linear dependence of $C(\nu)$ near ν_{BP} . A linear behavior of $C(\nu)$ for frequencies near that corresponding to the boson peak maximum can be seen for all the glasses. This linear behavior can be described by eq.(2). The constant B characterizes the relative contribution of two additive terms in eq.(2). Fig.6 presents a plot of $C(\nu)$ for seven glasses (SiO_2 , B_2O_3 , Se, CKN, $(\text{Ag}_2\text{O})_{0.14}(\text{B}_2\text{O}_3)_{0.86}$, PS, PC) plotted against scaled frequency (amplitudes of the $C(\nu)$ were normalized near $\nu/\nu_{BP} = 1$). For clarity, only data above $0.5\nu_{BP}$ are presented in this figure. Clear differences in $C(\nu)$ of the different glasses are observed at high frequencies. However, $C(\nu)$ tends to a master curve (universal frequency dependence) at frequencies below $\sim 1.5\nu_{BP}$. The universal behavior shown by the dashed line presents the dependence

$$C(\nu) \propto \nu/\nu_{BP} + 0.5 \quad (3)$$

The linear frequency dependence describes well the behavior of $C(\nu)$ found experimentally starting from the frequency $\sim 0.5\nu_{BP}$. The high frequency limit of this behavior varies from $1.5\nu_{BP}$ for SiO_2 and Se up to about $4\nu_{BP}$ for the PC glass.

However, there exists another group of glasses that does not follow the frequency behavior highlighted in Fig.6. The results for the other four glasses (PMMA, As_2S_3 , GeSe_2 , GeO_2) are presented in Fig.7. $C(\nu)$ for these glasses can be well described by a simple linear dependence with the constant B in eq.(2) having a value of zero.

Thus, all the glasses analyzed here are separated into two groups: those with $C(\nu) \propto \nu/\nu_{BP} + 0.5$ near the boson peak maximum (Fig.6), and another group with $C(\nu) \propto \nu$ (Fig.7). In the following we will refer to these two groups with the designation of "type-I" and "type-II", respectively.

Low-frequency behavior of $C(\nu)$ ($\nu < 0.5\nu_{BP}$). At least four glasses (SiO_2 , Se, PS and CKN) demonstrate superlinear frequency dependence in this spectral range. The low-frequency portions of $C(\nu)$ for these glasses are presented in Fig.8 on a log-log scale together with the function $C(\nu) \propto \nu/\nu_{BP} + 0.5$. The coupling coefficient varies superlinearly below some frequency $\sim 0.5\nu_{BP}$, deviating strongly from the extrapolation of linear behavior (Fig.8). The crossover frequency of a transition to superlinear behavior appears to be $\sim 0.3\nu_{BP}$ for SiO_2 and $\sim 0.5\nu_{BP}$ for Se, PS and CKN.

It is remarkable that these systems have significantly different microstructure and fragility. This suggests that superlinear frequency behavior for $\nu < (0.3 \div 0.5)\nu_{BP}$ may be general for various glasses. The fact that we did not observe the superlinear frequency behavior of $C(\nu)$ in other glasses can be explained by two reasons: either

the experimental data are not extended to low enough frequencies, or they are measured at temperatures that are not low enough and the presence of the fast relaxation at low frequencies masks the true vibrational behavior. The importance of the relaxation contribution even at temperature as low as $T = 15$ K can be demonstrated in the case of the B_2O_3 glass. Indeed, from Fig.1 of³¹ it is evident that the fast relaxation is not negligible at $T = 15$ K and dominates for $\nu < 3 \text{ cm}^{-1}$. Since the spectral shape of the fast relaxation spectrum in B_2O_3 does not depend on temperature³¹, we can subtract it from the Raman spectrum at $T = 15$ K using the spectrum of the fast relaxation determined in³¹. The Raman spectrum of B_2O_3 glass corrected in this way (by adjusting amplitude of the relaxational spectrum at the lowest points of the spectrum in Fig.1 of Ref.³¹) gives the coupling coefficient shown by the dotted line in Fig.8. This revised coupling coefficient depicts the superlinear behavior at $\nu < 0.5\nu_{BP}$.

High-frequency behavior of $C(\nu)$ ($\nu > 2\nu_{BP}$). Figs.6 and 7 show no universal behavior of the coupling coefficient in this frequency range. It varies from sublinear to strongly superlinear behavior for different glasses.

IV. DISCUSSION

The observation of the superlinear behavior of the coupling coefficient below some frequency $\nu < (0.3 \div 0.5)\nu_{BP}$ is very important. It has been shown that $C(\nu)$ for acoustic-like vibrations should increase $\sim \nu^2$. This prediction was obtained in the framework of different model approximations (see, for example, Refs.^{6,8,9}).

Basing on their experimental observations, the authors of Ref.²¹ suggested that the linear behavior of $C(\nu)$ can be extrapolated to the limit $\nu \rightarrow 0$ and $C(\nu = 0)$ has a nonvanishing value. The results of the present work show that this extrapolation is not correct and the character of the frequency dependence changes at lower ν , corresponding to the expectation that $C(\nu) \rightarrow 0$ when $\nu \rightarrow 0$. However, the existing experimental data do not allow one to establish the exact frequency dependence, and this topic still requires further investigation.

At higher frequencies, $C(\nu)$ demonstrates the universal linear behavior for type-I glasses (Fig.6). The glasses in this class vary significantly in structure, fragility, and ratio of the excess vibrations to the Debye level. There are many models that assume two different kinds of vibrations coexisting at frequencies around the boson peak: propagating and localized or quasilocal. For example, in the framework of the soft potential model⁴⁸ it is assumed that propagating waves have a Debye-like density of states and do not contribute to the Raman spectra, while excess vibrations are localized and have $C(\nu) = \text{const}$. The ratio of the excess vibrational density of states to the Debye level around the boson peak is ~ 4 in SiO_2 and ~ 0.4 in CKN³⁶, i.e. it differs up to 10 times. In that

respect, the observed universality of $C(\nu)$, obtained using the total density of vibrational states (Figures 6,7), supports an alternative idea that all vibrations around the boson peak are hybridized and can not be separated into propagating and localized.

In order to explain the observed universality of $C(\nu)$, significant theoretical work should be done. There are two complications in this problem: (i) there is no good approximation for the wavefunction of the vibrations around the boson peak; (ii) the scattering mechanism, i.e. the way how the vibrations modulate polarizability of the material, is not clear and might be different for different glasses. Below we consider a very simplistic model that might provide a qualitative description of the observed universal behavior of $C(\nu)$. One possible explanation for this behavior can be found in the framework of the approach of non-continuous glass nanostructure^{49–51}. The model assumes that the boson peak vibrations combine properties of both localized and extended excitations. At short distances (inside of a nanocluster), displacements of atoms are coherent and the wavefunction is similar to a vibration localized in the cluster. At longer distances, however, the vibrations start to have diffusive character (probably as in⁵²). Note that the spirit of this consideration is very similar to that of the model in⁵³.

For simplicity of discussion we will follow continuous medium approximation⁶. In this case the inelastic light scattering is caused by acoustic vibrations via the elasto-optic effect. The coupling coefficients for the Raman scattering of acoustic-type excitations is written as^{6,7}:

$$C(\nu) \propto \int \partial \vec{\tau} \langle P(0) P^*(\vec{\tau}) \rangle \langle s^\nu(0) s^{\nu*}(\vec{\tau}) \rangle \quad (4)$$

Here $s^\nu(\vec{\tau})$ is the strain of an acoustic vibration with frequency ν , $\langle \dots \rangle$ means configurational and statistical averaging, and $P(\vec{\tau})$ is the elasto-optic constant. Cross-correlations of $P(\vec{\tau})$ and $s^\nu(\vec{\tau})$ fluctuations are neglected for simplicity. Since the phonon mean free path is much shorter than the light wavelength, the exponential $\exp(i\vec{q}\vec{\tau})$ (where \vec{q} is the scattering wavevector of the experiment) is also neglected. The polarization indices are omitted for simplicity. We assume $\langle P(0) P^*(\vec{\tau}) \rangle \approx P^2$ and neglect contribution of the fluctuating part of the elasto-optic constant in the Raman coupling coefficient.

In the framework of the model considered, the integral of eq.(4) can be separated into two parts: the first is for the short distances, where the wavefunction of the vibration mimics the localized feature; the second one is for longer distances, where the wave function has diffusive character:

$$C(\nu) \propto \int_0^{|\vec{\tau}|=R} \partial \vec{\tau} \langle s^\nu(0) s^{\nu*}(\vec{\tau}) \rangle + \int_{|\vec{\tau}|=R}^{\infty} \partial r \langle s^\nu(0) s^{\nu*}(\vec{\tau}) \rangle \quad (5)$$

Here, R is the radius of the nanocluster. The wavefunction in the first term behaves as a localized vibration

and this is the case described in the Shuker-Gammon model⁷. Therefore, the first term is frequency independent. The diffusive character of the boson peak vibrations determines the frequency behavior of the second term in eq.(5). In Ref.⁵⁴, it was shown that the diffusive feature of acoustic vibrations leads to $C(\nu) \propto \nu$. Therefore, the second term in eq.(5) is proportional to frequency. Thus, the localized-extended character of the boson peak vibrations may be the reason for the linear frequency dependence of the Raman coupling coefficient.

According to eq.(5), the relative contributions to $C(\nu)$ of a frequency independent term and a term proportional to frequency reflects the relative weights of localized and extended part of the boson peak vibration. The result of Fig.6 means that at the boson peak maximum the ratio of the localized and extended parts is the same for these glasses.

However, the frequency independent contribution to $C(\nu)$ for some of glasses is negligibly small (Fig.7). In the framework of the considered model, it means that for these glasses either the vibrations have diffusive-like character even inside a nanocluster or this part of the wavefunction does not contribute to light scattering due to selection rules. We do not have a clear explanation for the observed difference and it remains a challenge for future investigations. At present we only show another hint that the peculiarity of type-II glasses may be related to localization of the vibrations. Indeed, if this is true one should expect that boson peak vibrations of type-II glasses are more extended than those of type-I glasses. This difference has to show up in vibration transport properties. Figure 9 presents the thermal conductivity of SiO₂, PS, Se, GeO₂, PMMA and As₂S₃ glasses (data from Refs.^{55–57}). The first three glasses are type-I and the next three are type-II. It is convenient to compare the pairs of glasses in which the two members of the pair have closely similar chemical nature but belong to different classes, for example, SiO₂ and GeO₂, PS and PMMA, As₂S₃ and Se. It appears (Fig.9) that glasses of different type (but of similar chemical nature) have comparable thermal conductivity at higher T but type-II glasses have higher thermal conductivity at the plateau. It is known that the plateau region in thermal conductivity corresponds to conductivity by vibrations around the boson peak. Thus, this comparison reveals weaker localization of the boson peak vibrations in type-II glasses and supports the above speculations. However, the question is far from settled and further investigations are needed in order to provide a microscopic explanation of the difference between the two types of glasses.

There are no universalities in the frequency dependence of $C(\nu)$ for $\nu > 2\nu_{BP}$. The high-frequency vibrations depend strongly on a particular atomic organization of a glass, its microstructure. A relation to peculiar microstructure may be a reason for different behaviors of $C(\nu)$ in this frequency range.

V. CONCLUSION

The Raman coupling coefficient, $C(\nu)$, is analyzed for the large number of glasses strongly different in their chemical structure and fragility. It is demonstrated that $C(\nu)$ has a universal linear frequency dependence near the boson peak maximum: $C(\nu) \propto \nu/\nu_{BP} + B$, with $B \sim 0.5$ for one group of glasses and $B \sim 0$ for the second group. The observed universality suggests that the vibrations around the boson peak have some universal properties for glasses with different structure. An explanation for the observed $C(\nu)$ is formulated in the framework of a model describing the vibrational wavefunction as a combination of localized and extended parts. We relate the difference in the behavior of $C(\nu)$ in the two groups of glasses to different localization properties of the vibrations on a short length scale. This suggestion agrees with the observation of different behavior of thermal conductivity in these two types of glasses. It is also shown that $C(\nu)$ has a superlinear behavior at frequencies below $\sim 0.3 \div 0.5 \nu_{BP}$. A sharp rise in mean free path of the vibrations with decrease in ν may be a reason for this fast decrease in $C(\nu)$. No universality is observed at higher frequencies (above $\sim 2\nu_{BP}$) suggesting that the particular atomic organization of glasses is important in this spectral range.

A. Acknowledgments

Help of S. Adichtchev in literature search is appreciated. This work was supported by RFFI Grants No 01-05-65066, 02-02-16112. A.P.S. acknowledges financial support from NSF (grant DMR-0080035) and NATO (grant PST.CLG.976150).

¹ "Amorphous Solids: Low-Temperature Properties", edited by W.A. Phillips (Springer, Berlin, 1981).

² U. Buchenau, N. Nücker, and A. J. Dianoux, Phys. Rev. Lett. **53**, 2316 (1984).

³ P. Benassi, M. Krisch, C. Masciovecchio, V. Mazzacurati, G. Monaco, G. Ruocco, F. Sette, and R. Verbeni, Phys. Rev. Lett. **77**, 3835 (1996).

⁴ M. Foret, E. Courtens, R. Vacher, and J. B. Suck, Phys. Rev. Lett. **77**, 3831 (1996).

⁵ U. Strom and P.C. Taylor, Phys. Rev. B **16**, 5512 (1977).

⁶ J. Jäckle, in "Amorphous Solids: Low-Temperature Properties", Edited by W.A. Phillips (Springer, Berlin, 1981).

⁷ R. Shuker and R.W. Gammon, Phys. Rev. Lett. **25**, 222 (1970).

⁸ A.J. Martin and W. Brenig, Phys. Status Solidi (b) **64**, 163 (1974).

- ⁹ E. Duval, L. Saviot, N. Surovtsev, J. Wiedersich, and A. J. Dianoux, Philos. Mag. B, v.79, 2051 (1999).
- ¹⁰ L. Saviot, E. Duval, N. Surovtsev, J. F. Jal, and A. J. Dianoux, Phys. Rev. B **60**, 18 (1999).
- ¹¹ G. Winterling, Phys. Rev. B **12**, 2432 (1975).
- ¹² A. P. Sokolov, U. Buchenau, W. Steffen, B. Frick, and A. Wischnewski, Phys. Rev. B **52**, R9815 (1995).
- ¹³ A. P. Sokolov, A. Kisliuk, D. Quitmann, and E. Duval, Phys. Rev. B **48**, 7692 (1993).
- ¹⁴ N. Ahmad, K. W. Hutt, and W. A. Phillips, J.Phys. C: Solid State Phys. **19**, 3765 (1986).
- ¹⁵ N. Ahmad and Matiulah, Sol. Stat. Comm. **76**, 433 (1990).
- ¹⁶ A. Fontana, F. Rocca, M.P. Fontana, B. Rosi, and A. J. Dianoux, Phys. Rev. B **41**, 3778 (1990).
- ¹⁷ B. Hehlen, E. Courtens, R. Vacher, A. Yamanaka, M. Kataoka, and K. Inoue, Phys. Rev. Lett. **84**, 5355 (2000).
- ¹⁸ D. Engberg, A. Wischnewski, U. Buchenau, L. Börjesson, A. J. Dianoux, A. P. Sokolov, and L. M. Torell, Phys. Rev. B **58**, 9087 (1998).
- ¹⁹ V. G. Karpov, M. I. Klinger, and F. N. Ignatiev, Sov. Phys. JETP **57**, 439 (1983).
- ²⁰ E. Courtens, M. Foret, B. Hehlen, and R. Vacher, Solid State Commun. **117**, 187 (2001).
- ²¹ A. Fontana, R. Dell'Anna, M. Montagna, F. Rossi, G. Viliani, G. Ruocco, M. Sampoli, U. Buchenau, and A. Wischnewski, Europhys. Lett. **47**, 56 (1999).
- ²² N. V. Surovtsev, Phys. Rev. E **64**, 061102 (2001).
- ²³ N. V. Surovtsev, T. Achibat, E. Duval, A. Mermet, and V. N. Novikov, J. Phys.: Condens. Matter **7**, 8077 (1995).
- ²⁴ A. Fontana, F. Rossi, G. Carini, G. D'Angelo, G. Tripodo, and A. Bartolotta, Phys. Rev. Lett. **78**, 1078 (1997).
- ²⁵ Y. Inamura, M. Arai, Yamamuro, A. Inaba, N. Kitamura, T. Otomo, T. Matsuo, S. M. Bennington, and A. C. Hannon, Physica B **263-264**, 299 (1999).
- ²⁶ U. Buchenau, M. Prager, N. Nucker, A. J. Dianoux, N. Ahmad, and W. A. Phillips, Phys. Rev. B **34**, 5665 (1986).
- ²⁷ N. V. Surovtsev, J. Wiedersich, V. N. Novikov, E. Rössler, and E. Duval, Phys. Rev. Lett. **82**, 4476 (1999).
- ²⁸ A. P. Sokolov, V. N. Novikov, and B. Strube, Europhys. Lett. **38**, 49 (1997).
- ²⁹ E. Pérez-Enciso, M. A. Ramos, and S. Vieira, Phys. Rev. B **56**, 32 (1997).
- ³⁰ G. K. White, S. J. Collocott, and J. S. Cook, Phys. Rev. B **29**, 4778 (1984).
- ³¹ N. V. Surovtsev, J. A. H. Wiedersich, E. Duval, V. N. Novikov, E. Rössler, and A. P. Sokolov, J. Chem. Phys. **112**, 2319 (2000).
- ³² N. V. Surovtsev, J. Wiedersich, A. E. Batalov, V. N. Novikov, M. A. Ramos, and E. Rössler, J. Chem. Phys. **113**, 5891 (2000).
- ³³ J.C. Lasjaunias and R. Maynard, J. Non-Cryst. Solids **6**, 101 (1971).
- ³⁴ R.C. Zeller and R.O. Pohl, Phys. Rev. B **6**, 2029 (1971).
- ³⁵ W. A. Phillips, U. Buchenau, N. Nücker, A.-J. Dianoux, and W. Petry, Phys. Rev. Lett. **63**, 2381 (1989).
- ³⁶ A. P. Sokolov, R. Calemczuk, B. Salce, A. Kisliuk, D. Quitmann, and E. Duval, Phys. Rev. Lett. **78**, 2405 (1997).
- ³⁷ N. V. Surovtsev, J. A. H. Wiedersich, V. N. Novikov, E. Rössler, and A. P. Sokolov, Phys. Rev. B **58**, 14888 (1998).
- ³⁸ M. Russina, F. Mezei, R. Lechner, S. Longeville, and B.

- Urban, Phys. Rev. Lett. **84**, 3630 (2000).
- ³⁹ V. K. Malinovsky, V. N. Novikov, and A. P. Sokolov, Phys. Lett. A **153**, 63 (1991).
- ⁴⁰ G. Carini, G. D'Angelo, G. Tripodo, A. Fontana, A. Leonardi, G. A. Saunders, and A. Brodin, Phys. Rev. B **52**, 9342 (1995).
- ⁴¹ W. A. Kamitakahara, R. L. Cappelletti, P. Boolchand, B. Halfpap, F. Gompf, D. A. Neumann, and H. Mutka, Phys. Rev. B **44**, 94 (1991).
- ⁴² S. Sugai, Phys. Rev. B **35**, 1345 (1987).
- ⁴³ G. Tripodo, G. D'Angelo, G. Carini, A. Bartolotta, A. Fontana, and F. Rossi, J. Phys.: Condens Matter **11**, A229 (1999).
- ⁴⁴ B. V. Lebedev, N. N. Smirnova, N. K. Kozyreva, A. I. Kirilin, and V. V. Korchak, Dokl. Akad. Nauk USSR **270**, 129 (1983).
- ⁴⁵ V. N. Novikov, A. P. Sokolov, B. Strube, N. V. Surovtsev, E. Duval, and A. Mermet, J. Chem. Phys. **107**, 1057 (1997).
- ⁴⁶ N. V. Surovtsev, A. Mermet, E. Duval, and V. N. Novikov, J. Chem. Phys. **104**, 6818 (1996).
- ⁴⁷ A. Mermet, N. V. Surovtsev, E. Duval, J. F. Jal, J. Dupuy-Philon, and A. J. Dianoux, Europhys. Lett. **36**, 277 (1996).
- ⁴⁸ D. A. Parshin, Phys. Solid State **36**, 991 (1994).
- ⁴⁹ A. P. Sokolov, A. Kisliuk, M. Soltwisch, and D. Quitmann, Phys. Rev. Lett. **69**, 1540 (1992).
- ⁵⁰ E. Duval, A. Boukenter, and T. Achibat, J. Phys.: Cond. Matter **2**, 10227 (1990).
- ⁵¹ S. R. Elliot, Europhys. Lett. **19**, 201 (1992).
- ⁵² J. Fabian and P.B. Allen, Phys. Rev. Lett. **77**, 3839 (1996).
- ⁵³ E. Duval and A. Mermet, Phys. Rev. B **58**, 8159 (1998).
- ⁵⁴ V. N. Novikov, Proc. of XIV-th Int. Conf. on Raman Scattering, Eds. N.-T. Yu and X.-Y. Li (John Wiley&Sons, NY, 1994) p.766.
- ⁵⁵ C. C. Yu and J. J. Freeman, Phys. Rev. B **36**, 7620 (1987).
- ⁵⁶ J. E. Graebner, B. Golding, and L. C. Allen, Phys. Rev. B **34**, 5696 (1986).
- ⁵⁷ D. G. Cahill and R. O. Pohl, Phys. Rev. B **35**, 4067 (1987).

Table 1. Boson peak position, defined as the position of maximum of g/ν^2 .

	glass	BP position [cm ⁻¹]
1	SiO ₂	33.5
2	B ₂ O ₃	18
3	(Ag ₂ O) _{0.14} (B ₂ O ₃) _{0.86}	22.5
4	Se	12
5	As ₂ S ₃	16.5
6	CKN	20.5
7	GeSe ₂	10
8	GeO ₂	27
9	PC	11
10	PS	11.5
11	PMMA	12.5

Figure 1. Frequency dependence of the coupling coefficient $C(\nu)$ for SiO_2 glass. Closed circles are polarized Raman scattering data from Ref.²⁷ (open circles are explained in the text), thick solid line is the coupling coefficient for depolarized Raman data of Ref.²⁸. Thin line is $\propto \nu$ behavior. Triangles are $C(\nu)$ data from Ref.²¹. Squares are $C(\nu)$ data from Ref.¹². Inset shows the low-frequency ($10\text{-}40\text{ cm}^{-1}$) part of $C(\nu)$ in details.

Figure 2. Frequency dependence of the coupling coefficient $C(\nu)$ for B_2O_3 glass. Solid line is $C(\nu)$ found for the density of states evaluated from the specific heat data. Circles are $C(\nu)$ from Ref.¹⁸. Inset shows the low-frequency ($< 30\text{ cm}^{-1}$) part of $C(\nu)$ in details.

Figure 3. Frequency dependence of the coupling coefficient $C(\nu)$ for CKN and Se glasses: triangles and circles correspond to density of states evaluated from specific heat data, dotted and solid lines is for density of states from inelastic neutron scattering (CKN and Se, respectively). Inset shows the low frequency range in details.

Figure 4. Frequency dependence of the coupling coefficient $C(\nu)$ for As_2S_3 (circles), GeO_2 (triangles), GeSe_2 (thin line) and $(\text{Ag}_2\text{O})_{0.14}(\text{B}_2\text{O}_3)_{0.86}$ (thick line) glasses. Inset shows the low-frequency part of $C(\nu)$ in details.

Figure 5. Frequency dependence of the coupling coefficient $C(\nu)$ for polymeric glasses: PS - thin line corresponds to the density of states from neutron scattering experiment (data from Ref.¹²), circles to the one evaluated from specific heat data; PC - triangles (data from Ref.¹⁰), PMMA - thick solid line corresponds to the density of states from neutron scattering experiment (data from Ref.⁴⁷), squares to the one evaluated from specific heat data. Inset shows the low-frequency part of $C(\nu)$ in details.

Figure 6. Frequency dependence of the coupling coefficient $C(\nu)$ for glasses: SiO_2 , B_2O_3 , Se, CKN, $(\text{Ag}_2\text{O})_{0.14}(\text{B}_2\text{O}_3)_{0.86}$, PS, PC, versus scaled frequency ν/ν_{BP} . Only region above $0.5\nu_{BP}$ is presented. Numbers of lines correspond to the numbers in the Table 1. Triangles are $(\text{Ag}_2\text{O})_{0.14}(\text{B}_2\text{O}_3)_{0.86}$, circles are CKN data. Dashed line is a fit $C(\nu) \propto \nu/\nu_{BP}+0.5$. Inset shows the low-frequency part of $C(\nu)$ in details.

Figure 7. Frequency dependence of the coupling coefficient $C(\nu)$ for glasses: PMMA (dotted line), As_2S_3 (triangles), GeSe_2 (solid line), GeO_2 (circles) versus scaled frequency ν/ν_{BP} . Dashed line is a fit $C(\nu) \propto \nu$. Inset shows the low-frequency part of $C(\nu)$ in details.

Figure 8. The low-frequency part of the coupling coefficient $C(\nu)$ for glasses: SiO_2 (solid line), Se (triangles), PS (squares), CKN (circles) in logarithmic scale. Dashed line is $C(\nu) \propto \nu/\nu_{BP}+0.5$. Dotted line is $C(\nu)$ for the corrected Raman spectrum of B_2O_3 glass as explained in the text.

Figure 9. Thermal conductivity of SiO_2 (solid line), GeO_2 (dotted line), PMMA (open circles), PS (solid circles), As_2S_3 (open triangles), Se (solid triangles). Data

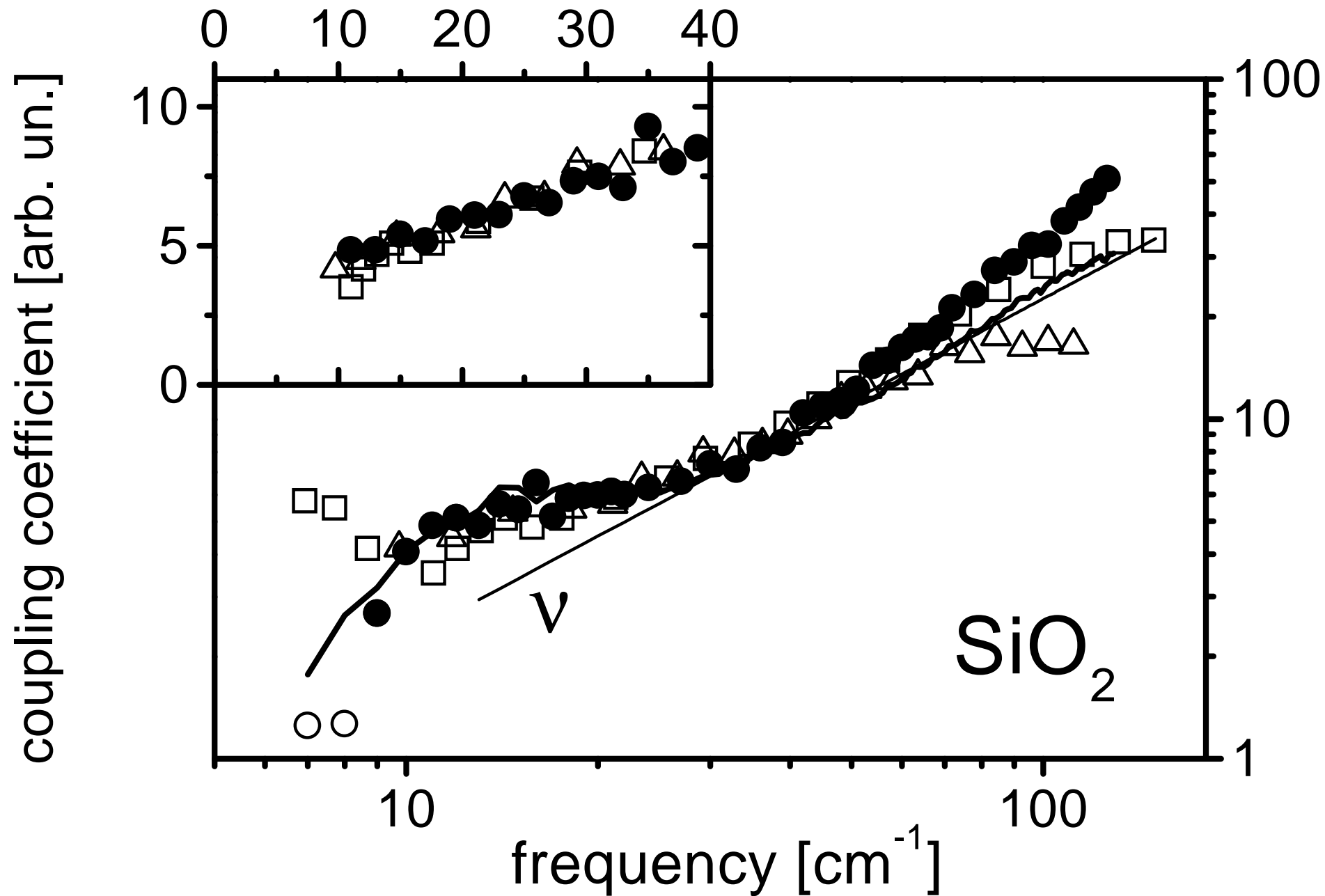


Figure 1.

N.V. Surovtsev, A.P. Sokolov "Frequency behavior of Raman coupling coefficient in glasses"

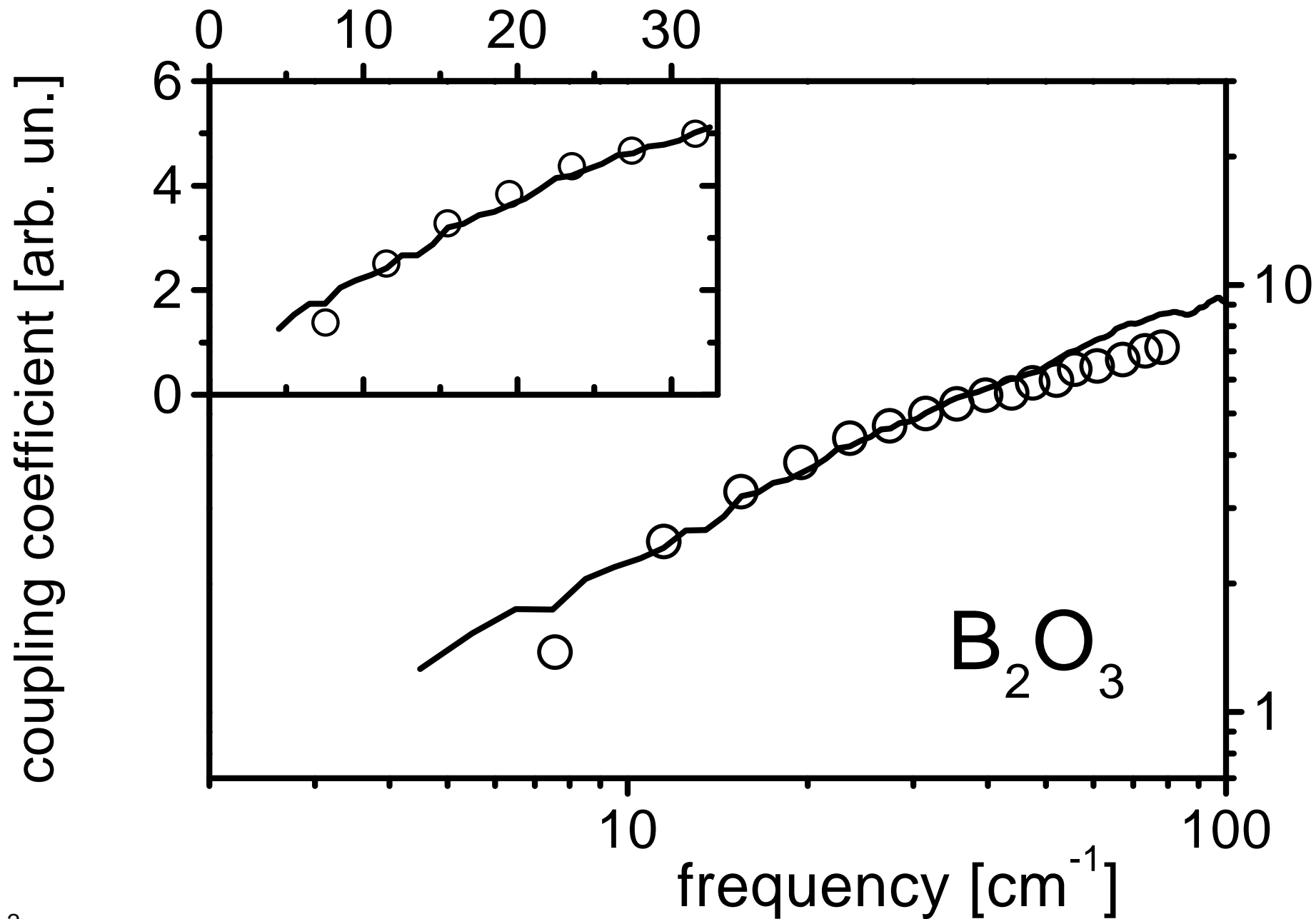


Figure 2.

N.V. Surovtsev, A.P. Sokolov "Frequency behavior of Raman coupling coefficient in glasses"

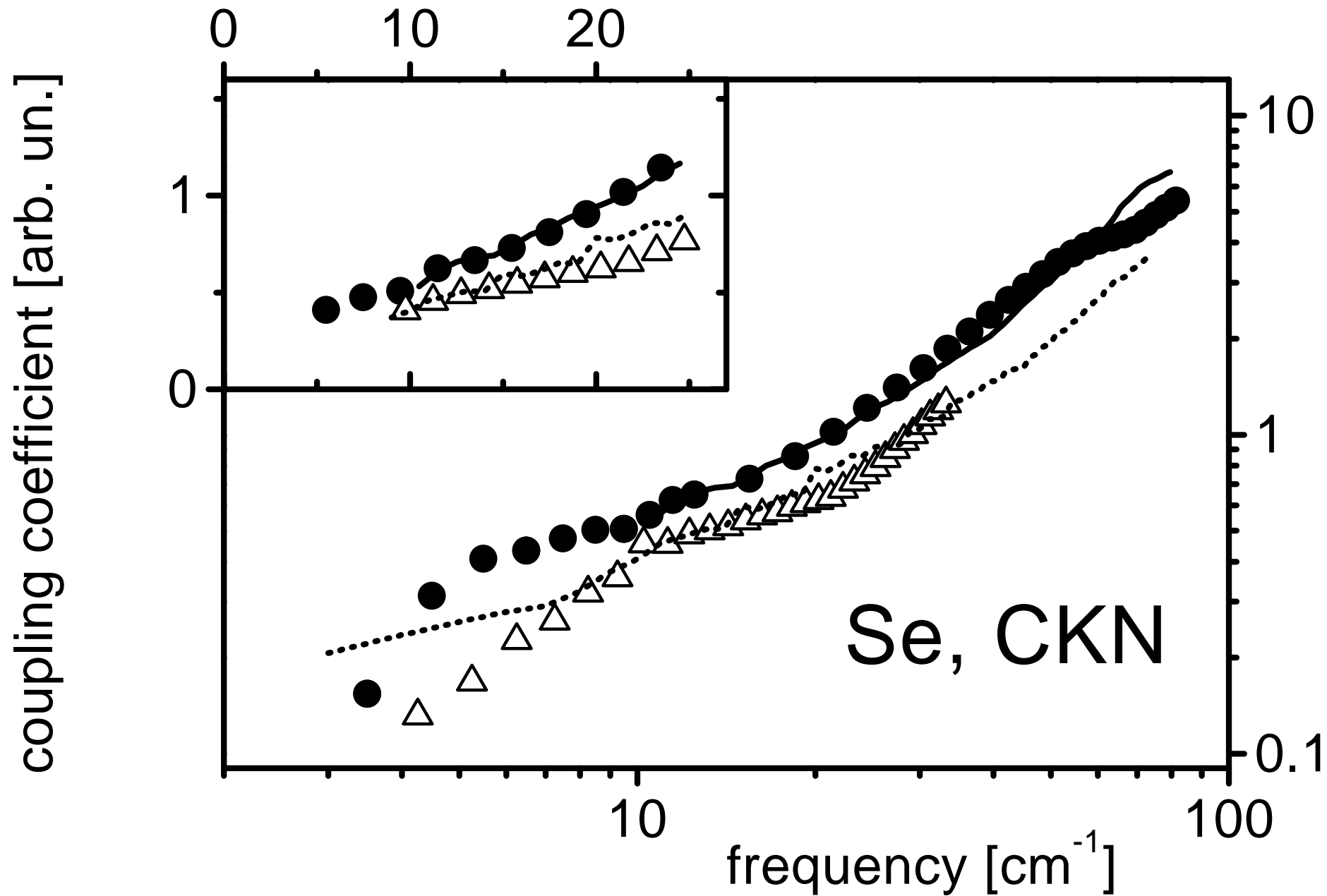


Figure 3.

N.V. Surovtsev, A.P. Sokolov "Frequency behavior of Raman coupling coefficient in glasses"

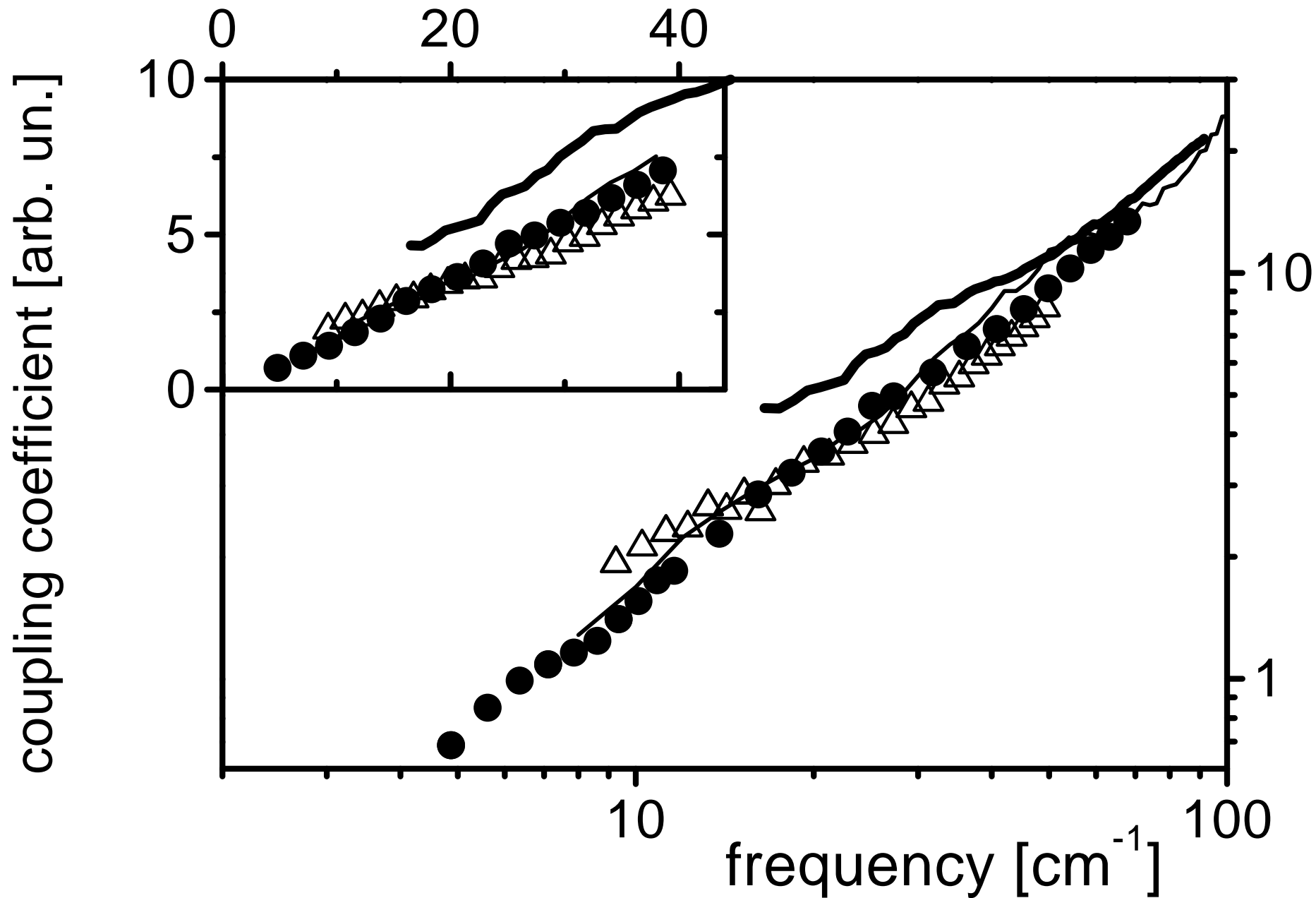


Figure 4.

N.V. Surovtsev, A.P. Sokolov "Frequency behavior of Raman coupling coefficient in glasses"

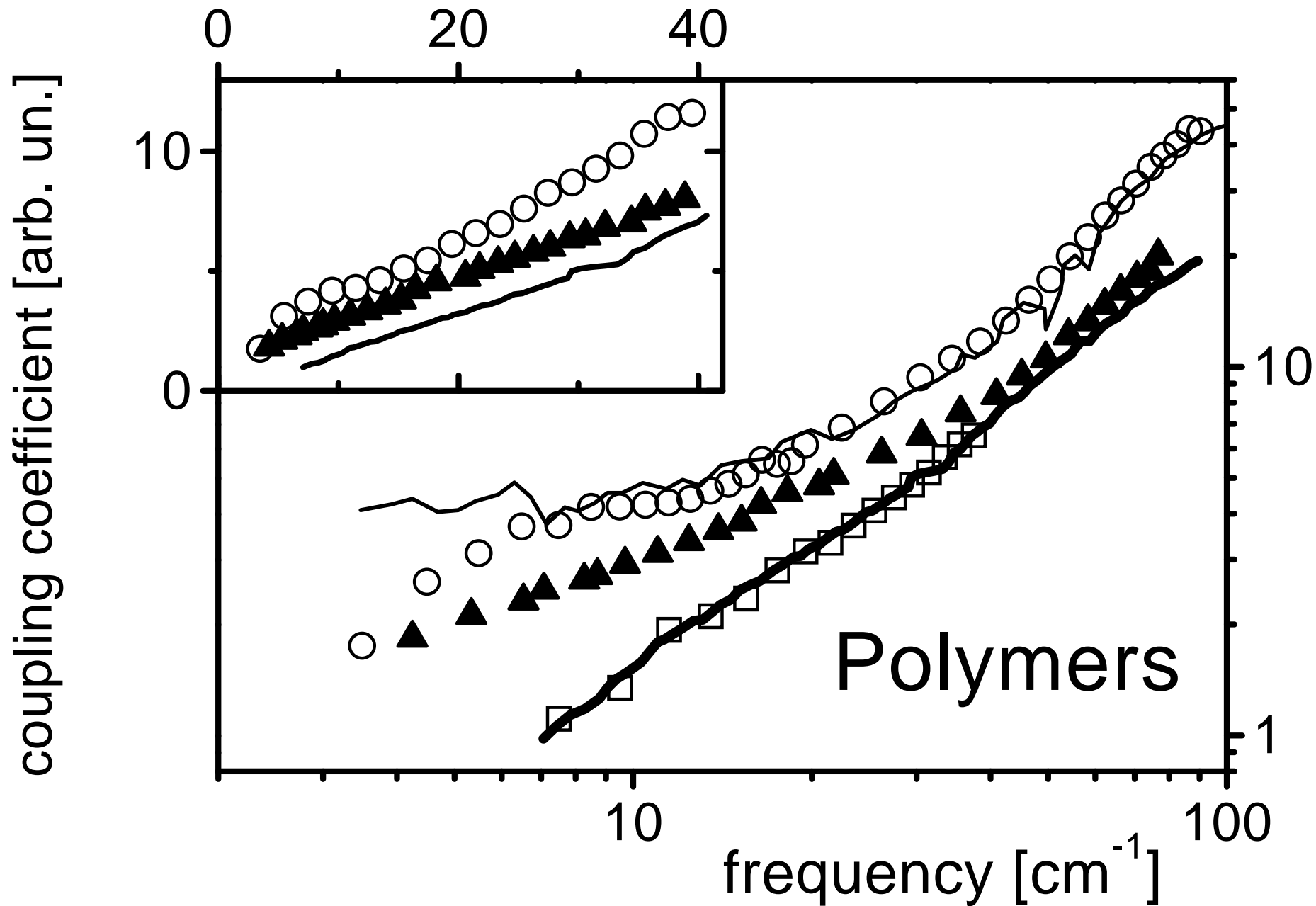


Figure 5.

N.V. Surovtsev, A.P. Sokolov "Frequency behavior of Raman coupling coefficient in glasses"

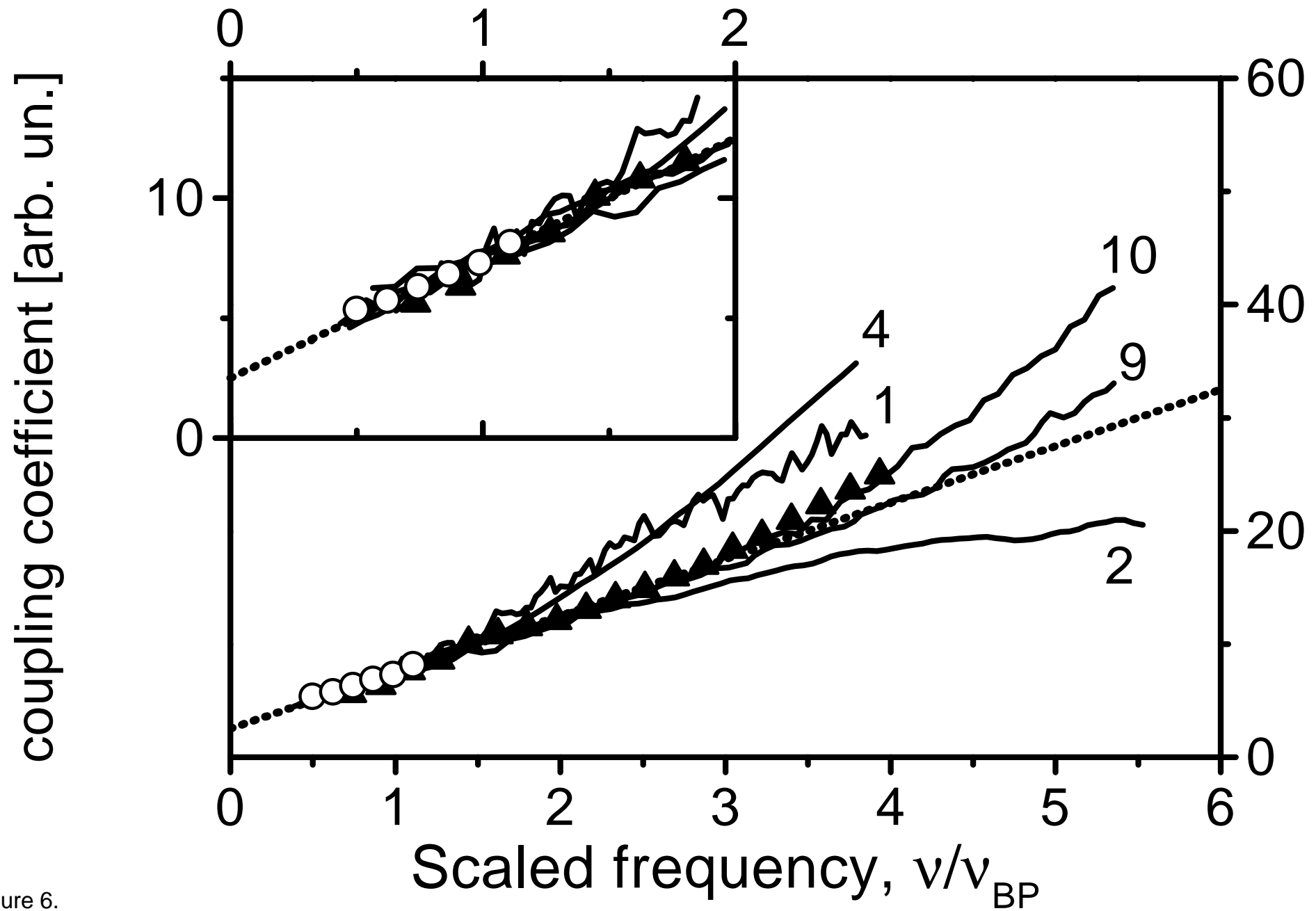


Figure 6.

N.V. Surovtsev, A.P. Sokolov "Frequency behavior of Raman coupling coefficient in glasses"

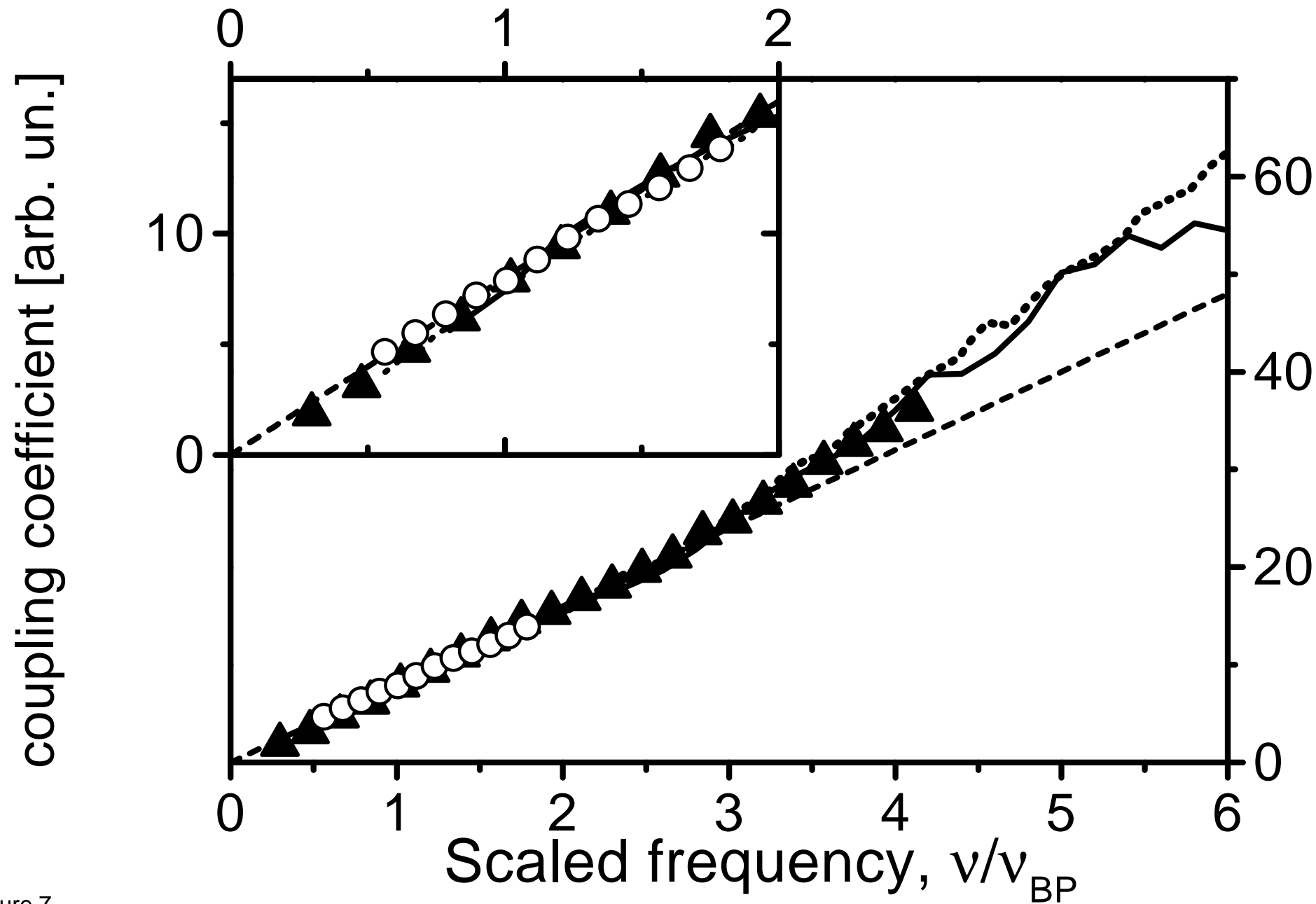


Figure 7.

N.V. Surovtsev, A.P. Sokolov "Frequency behavior of Raman coupling coefficient in glasses"

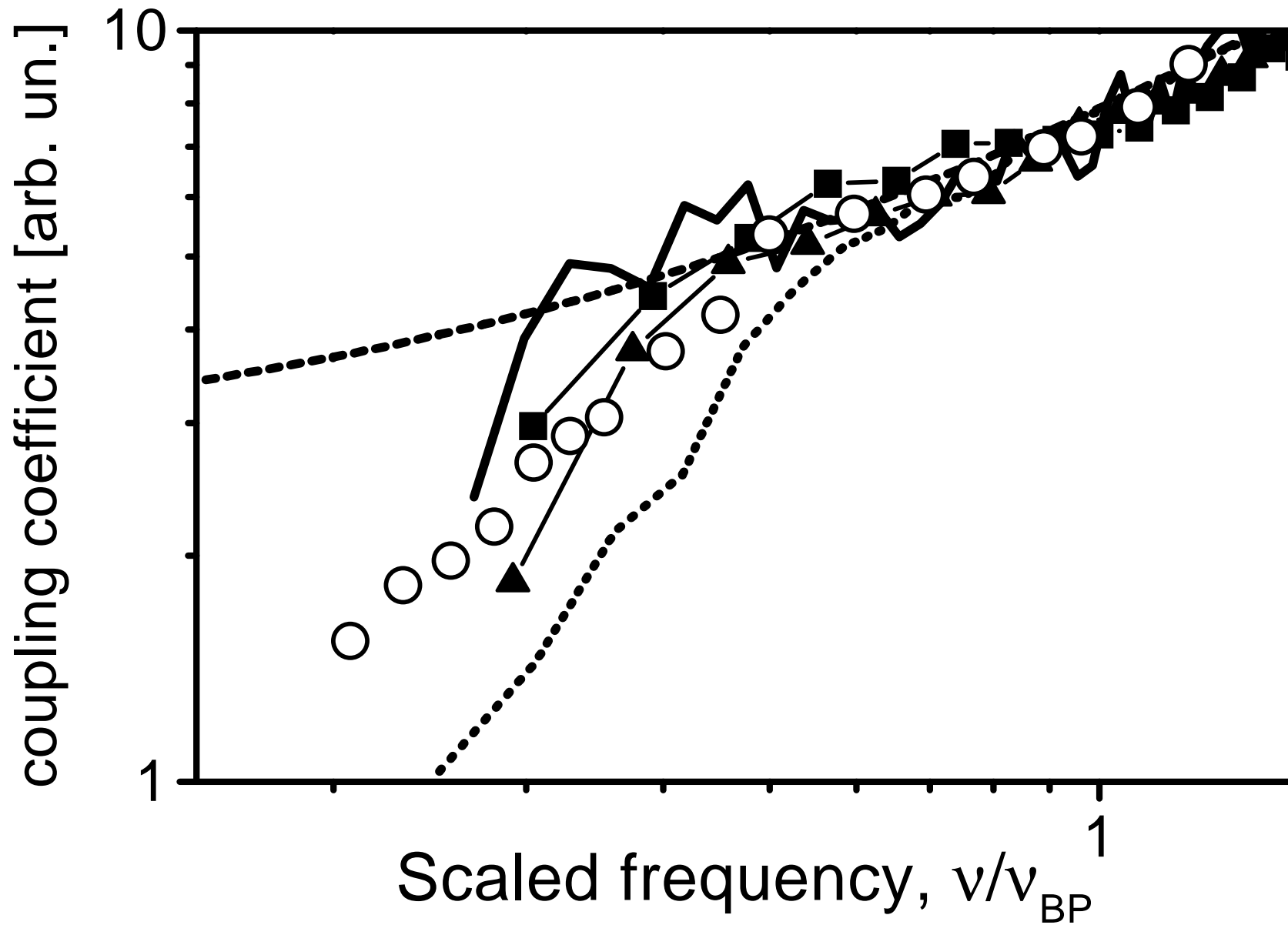


Figure 8.

N.V. Surovtsev, A.P. Sokolov "Frequency behavior of Raman coupling coefficient in glasses"

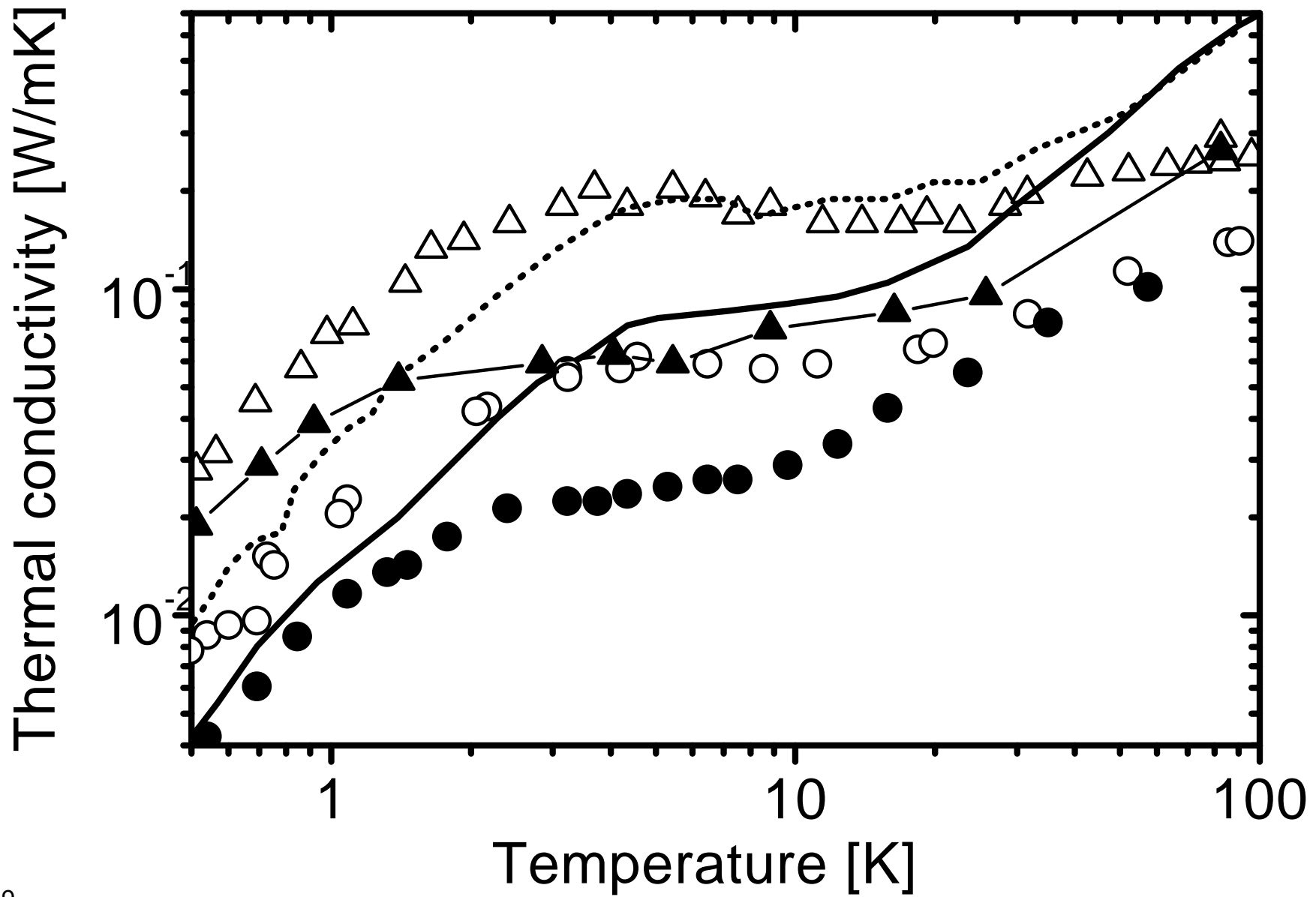


Figure 9.

N.V. Surovtsev, A.P. Sokolov "Frequency behavior of Raman coupling coefficient in glasses"